

Dispersions of Hollow and Bamboo-Like Multiwalled Carbon Nanotubes in Polyethyleneimine: Critical Analysis of the Preparation Conditions and Applications for Electrochemical Sensing

Marcos Eguílaz,^[a] Nancy F. Ferreyra,^{*,[a]} and Gustavo A. Rivas^{*,[a]}

Abstract: This work is focused on the critical analysis of the influence of the experimental conditions on the efficient dispersion of hollow-type (hMWCNT) and bamboo-like (bMWCNT) multiwall carbon nanotubes with polyethyleneimine (PEI). Spectroscopic and electrochemical studies demonstrated that the adequate combination of optimized ultracavitation and centrifugation is essential to obtain successful dispersions. The selected conditions

were 1.0 mg mL⁻¹ hMWCNT in 3.0 mg mL⁻¹ PEI sonicated with a sonicator probe operating at 50 % of amplitude for 300 s and centrifuged at 9000 rpm for 15 min. Bamboo-like multiwall carbon nanotubes were faster exfoliated and glassy carbon electrodes (GCE) modified with the resulting dispersion allowed the amperometric detection of hydrogen peroxide at lower potentials (0.100 V) with a detection limit of 5.5 μ M.

Keywords: Multiwalled carbon nanotubes • Carbon nanotubes dispersion • Electrochemical sensors

1 Introduction

The preparation of electrochemical sensors and biosensors based on nanomaterials has received increasing attention in the last years due to their exceptional physical and chemical properties [1]. In particular, carbon nanotubes (CNTs) have demonstrated to play a relevant role in the field of electrochemical (bio)sensors due to their unique structure, high thermal and chemical stability, and excellent electronic properties [1,2].


CNTs consist of a graphene sheet rolled up to form one tube (single-walled carbon nanotubes, SWCNTs) or multiple concentric tubes (multi-walled carbon nanotubes, MWCNTs) of nanometric diameter and different length [3]. In the case of MWCNTs, depending on the preparation conditions, there are different morphological variations such as “hollow tube” (hMWCNT), “bamboo-like” (bMWCNT) and “herringbone” (heMWCNT) [4]. hMWCNTs are ideally defect-free, while bMWCNTs present a large number of transverse walls at regular intervals along the nanotube, resulting in edge-planes of graphene regularly located along the tubes [5]. Since the edge-planes of graphene are more electroactive than the walls, bMWCNTs are expected to have active sites at regular intervals. Matsubara and Waki [6] demonstrated that the reduction of oxygen is facilitated at bMWCNTs compared to hMWCNTs, attributing this effect to the introduction of pentagonal defects into the hexagonal network that produces a positive curvature and bamboo-shaped morphology. Shanmugam and Gedanken [7,8] reported that the electrodes modified with bMWCNT present faster electron transfer compared to those containing hMWCNTs due to the better wettability and the presence

of edge-plane-like defects and oxygenated functional groups. Primo et al. [9] have demonstrated the advantages of bMWCNTs over hMWCNTs dispersed in calf-thymus double stranded DNA for the electrooxidation of hydrogen peroxide. bMWCNTs have been also used for the immobilization of biomolecules [10] and metal nanoparticles [11,12].

One of the major problems of using CNTs for the preparation of electrochemical (bio)sensors is the lack of solubility of this material in common solvents mainly due to the strong van der Waals interactions between the nanotubes walls that produce their aggregation in bundles [13,14].

The functionalization of CNTs has received considerable attention as strategy to minimize these interactions and improve the compatibility with the solvent [15–19]. Basically, there are two types of functionalization, covalent and non-covalent. The covalent approach produces alterations in the π system of CNTs and, thereby, in their intrinsic electronic properties [15]. Non-covalent functionalization has been widely used since it allows a successful derivatization of CNTs without disturbing their π -conjugated structure [20]. One of the most interesting

[a] M. Eguílaz, N. F. Ferreyra, G. A. Rivas
INFIQC. Departamento de Físico Química, Facultad de Ciencias Químicas, Universidad Nacional de Córdoba
Ciudad Universitaria, 5000 Córdoba, Argentina
phone: +54-351-5353866; fax: +54-351-4334188
*e-mail: ferreyra@fcq.unc.edu.ar
grivas@fcq.unc.edu.ar
mrubio@fcq.unc.edu.ar

 Supporting information for this article is available on the WWW under <http://dx.doi.org/10.1002/elan.201400298>.

non-covalent alternatives is based on the functionalization with polymers through the formation of supramolecular complexes with the surface of CNTs [9,17–21]. Several polymers have been used for this purpose [13,22–24]. Our group has been pioneer in the successful dispersion of MWCNTs with polyethyleneimine (PEI) using a sonicator bath [25] and in the development of electrochemical (bio)sensors to quantify different analytes [26–28]. PEI presents several advantages that make it very attractive to functionalize MWCNTs. In fact, it is highly efficient as n-doping agent due to their amine groups, it presents one of the highest densities of amine groups among all the polymers [29], it provides a hydrophilic environment that protects the biomolecules, especially in organic media. In addition, PEI-grafted CNTs have demonstrated important advantages as carriers for gene delivery with notable advantages over other polymers [30].

The interaction of CNTs with polymers produces a reorganization of the nanostructures by hiding the hydrophobic surface of the nanotubes walls and exposing to the solvent the hydrophilic residues of the polymer that interacts with CNTs [31]. Therefore, the separation of the tightly bound bundles by adsorption of polymers onto the side-walls of CNTs requires a significant energy input. In this sense, the sonication has been adopted as universal procedure to separate the nanotube bundles [32–34]. The strong shear force that enables the disaggregation of the bundles comes from the cavitation process, which entails bubble formation, growth and collapse [35]. The energy received by the sample depends on many factors connected to the characteristics of the solvent, the sonication parameters (i.e. applied intensity, ultrasound frequency and time), and the container geometry [33–34]. In general, the sonication treatment is performed by using ultrasonic baths or sonicator probes. Since sonicator probes typically operate at lower frequencies than the ultrasonic baths, they produce larger cavitation bubbles and deliver higher energy, decreasing the preparation time of the dispersions and improving their quality [35].

The aim of this work is to critically evaluate the influence of the preparation conditions of PEI-MWCNTs dispersions on their efficiency and on the response of glassy carbon electrodes (GCE) modified by drop-coating with the resulting MWCNTs-PEI dispersions. At variance of our previous publication [25], in this work we propose the use of a sonicator probe, followed by ultracentrifugation to eliminate biggest aggregates of CNT. In the following sections we discuss the effect of the sonication time, acoustic amplitude, ultrasonic frequency, solvent, PEI concentration, centrifugation, and nature of MWCNTs (hMWCNTs versus bMWCNTs) on the effectiveness of the dispersions by using UV-vis spectroscopy, cyclic voltammetry and amperometry. The sensing application of the resulting electrodes is also discussed in connection with the quantification of hydrogen peroxide. We also compare the electrochemical response obtained with the dispersion prepared with sonicator bath and sonicator horn.

2 Experimental

2.1 Chemicals and Solutions

Hollow-type multiwalled carbon nanotubes (hMWCNTs, diameter (30 ± 15) nm, length 1–5 μm and purity higher than 95 %), and bamboo-like multiwalled carbon nanotubes (bMWCNTs, diameter (30 ± 10) nm, length 1–5 μm and 98.92 % purity) were supplied from NanoLab (USA). The CNTs were used pristine without chemical purification.

Hydrogen peroxide (30 % v/v aqueous solution), ascorbic acid (AA), ethanol, hydroquinone (HQ), NaH_2PO_4 and Na_2HPO_4 were purchased from Baker. Polyethyleneimine (PEI, 50 % w/v, average MW 750000) was obtained from Sigma. All chemicals were of analytical grade and were used without further purification. The mouthwash sample (Colgate Plax Whitening), was obtained in a local drugstore.

PEI solutions were prepared in water or ethanol/water (50 % v/v and 70 % v/v). A 0.050 M phosphate buffer solution pH 7.40 was employed as supporting electrolyte. Ultrapure water ($\rho = 18.2 \text{ M}\Omega\text{cm}$) from a Millipore-MilliQ system was used for preparing all the solutions.

2.2 Apparatus

Sonication treatments were carried out with a sonicator probe VCX 130W (Sonics and Materials, Inc.) of 20 kHz frequency with a titanium alloy microtip (3 mm diameter) and an ultrasonic bath (TESTLAB, model TB04) of 40 kHz frequency and 160 W of nominal power. An Allegra 21 ultracentrifuge (Beckman Coulter) with a F2402H rotor was used to centrifuge the samples after sonication.

Electrochemical experiments were carried out with CHI 600D (CHI Instruments) and TEQ_04 potentiostats using three-electrodes cells. Unmodified glassy carbon electrodes (GCE, CH Instruments, 3 mm diameter) and glassy carbon electrodes modified with MWCNTs dispersed in PEI were used as working electrodes. A platinum wire and a Ag/AgCl, 3 M NaCl (BAS, Model RE-5B) were used as auxiliary and reference electrodes, respectively. All potentials are referred to this electrode. A magnetic stirrer under controlled speed provided the convective transport during the amperometric measurements.

UV-vis absorption spectra were obtained with a Shimadzu UV-1700 Pharma spectrophotometer using a quartz cuvette of 1 mm path length. The spectra of the dispersions were obtained before and after centrifugation of the samples. Noncentrifuged samples were allowed to settle for 30 min after sonication to discard CNTs macroaggregates. Proper dilution of the supernatant was performed before obtaining the UV-vis spectra.

Scanning Electron Microscopy (SEM) images were obtained with a Field Emission Gun Scanning Electron Microscope (FE-SEM, Zeiss, SIGMA model) equipped with secondary and back-scattered electron detectors. For this

purpose, samples were prepared by drop-coating of MWCNT dispersions onto GCE disks and air dried.

2.3 Preparation of the Modified Electrodes

2.3.1 Preparation of MWCNTs-PEI Dispersions

hMWCNTs-PEI and bMWCNTs-PEI dispersions were prepared by sonicating 1.0 mg of hMWCNTs or bMWCNTs with 1.0 mL of a PEI solution (3.0 mg mL^{-1} in water) using a sonicator probe (amplitude of 50%) for 300 s (4.25 W). During sonication the samples were kept in an ice-bath. After this treatment, the samples were centrifuged at 9000 rpm for 15 min. The supernatant was used for the modification of the electrodes and for the spectroscopic experiments.

2.3.2 Preparation of GCE Modified with MWCNTs-PEI Dispersions

GCE surfaces were polished with alumina slurries of 1.0, 0.3 and $0.05 \mu\text{m}$ for 1 min each, rinsed thoroughly with deionized water and sonicated for 30 s in water. The electrodes were carefully dried under a N_2 stream. An aliquot of $10 \mu\text{L}$ of hMWCNT-PEI or bMWCNT-PEI dispersions was dropped onto the glassy carbon surfaces and the solvent was evaporated at room temperature for 60 min. The electrodes modified with the optimized hMWCNTs-PEI or bMWCNTs-PEI dispersions were electrochemically treated by successively scanning the potential between -0.200 V and 0.800 V at 0.100 V s^{-1} (15 cycles) in a 0.050 M phosphate buffer solution pH 7.40 to oxidize the excess of PEI, stabilize the surfaces and obtain better reproducibility.

2.4 Procedure

The electrochemical experiments were performed in a 0.050 M phosphate buffer solution pH 7.40. Cyclic voltammetry (CV) was carried out in the range between -0.200 V and 0.800 V at a scan rate of 0.100 V s^{-1} . Amperometric experiments were performed in stirred solutions by applying the desired potential and allowing the transient current to reach a steady-state value prior to the addition of the analyte and the subsequent current monitoring. All experiments were conducted at room temperature.

The electroactive area of the different electrodes was obtained by CV using a $5.0 \times 10^{-4} \text{ M}$ hydroquinone solution as redox probe. The areas were calculated using the Randles equation considering a diffusion coefficient of HQ of $1.2 \times 10^{-5} \text{ cm}^2 \text{ s}^{-1}$ [36].

2.5 Determination of H_2O_2 in Mouthwash Samples

A mouthwash was used to evaluate the analytical performance of the proposed sensors. The stock solutions were prepared in 0.050 M phosphate buffer solution pH 7.40. Aliquots of $25 \mu\text{L}$ of 1:4 diluted stock solution (in the

case of GCE/hMWCNT-PEI) or $50 \mu\text{L}$ of 1:1 diluted stock solution (in the case of bMWCNT-PEI) were transferred to the electrochemical cell containing 5.0 mL of 0.050 M phosphate buffer solution pH 7.40 and the determinations of hydrogen peroxide were performed by amperometry at the selected potential. The hydrogen peroxide content was determined by using the standard addition method.

3 Results and Discussion

3.1 Influence of the Experimental Conditions on the Efficiency of hMWCNTs-PEI Dispersions and on the Electrochemical Behavior of GCE Modified with hMWCNT-PEI

One of the main goals when developing CNTs-based electrochemical sensors is to efficiently disperse the nanotubes in order to obtain a uniform and stable film once deposited onto the electrode surface. In this section, we discuss the influence of solvent, PEI concentration, sonication time, acoustic amplitude, ultrasound frequency and centrifugation conditions, on the efficiency of the dispersion of hMWCNTs and on the performance of GCE modified with the resulting dispersions.

3.1.1 Effect of the Solvent

Since the number of cavitation events and bubbles formation can change with the solvent [33], the cavitation process is strongly dependent on the nature of the solvent. To investigate this effect, we disperse 1.0 mg mL^{-1} of hMWCNTs in 1.0 mg mL^{-1} PEI prepared in water, 50:50 v/v ethanol/water and 70:30 v/v ethanol/water by sonication for 300 s using an amplitude of 50%, followed by a centrifugation step at 9000 rpm for 15 min. The macroscopic observation of the different supernatants indicated that the amount of dispersed CNTs was higher when using PEI prepared in 50/50 v/v ethanol/water (not shown). In order to rationalize these observations and considering that: i) the individual nanotubes have strong absorption in the UV region; ii) the maximum absorbance of these individual nanotubes occurs at 265 nm (Abs_{265}) due to 1D van Hove singularities [37–39]; iii) the aggregates of CNTs are hardly active in this frequency region [40,41], we obtained UV spectra of the supernatant of hMWCNT-PEI dispersions. These spectra allowed us to know the amount and stability of individually dispersed hMWCNTs. The Abs_{265} of the supernatants for dispersions prepared in water, 50:50 v/v ethanol/water and 70:30 v/v ethanol/water (diluted twice) were 0.74, 1.32 and 0.63, respectively, indicating that the highest amount of exfoliated nanotubes is obtained using 50:50 v/v ethanol/water as solvent.

We also evaluate the voltammetric response of $1.0 \times 10^{-3} \text{ M}$ AA at GCE/hMWCNTs-PEI modified with the different dispersions. As Figure 1 shows, in spite of the results obtained by UV spectroscopy, at GCE modified

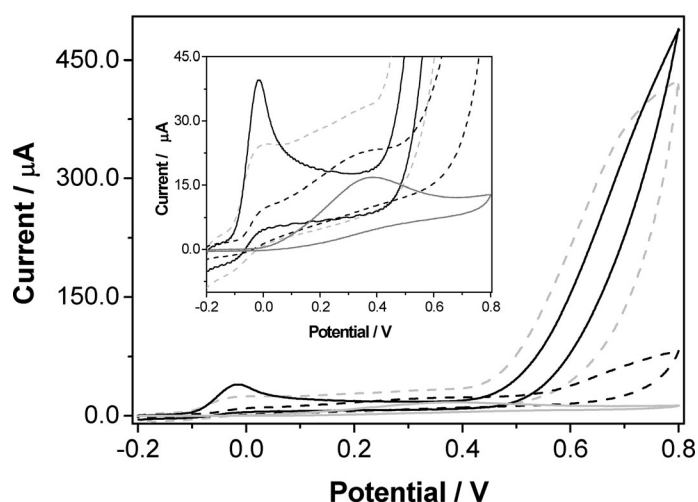


Fig. 1. Cyclic voltammograms of 1.0×10^{-3} M AA at GCE (---) and GCE modified with hMWCNTs-PEI using different solvents. The dispersions were obtained by mixing 1.0 mg mL^{-1} hMWCNTs in 1.0 mg mL^{-1} of PEI prepared in water (—), 50:50 v/v ethanol/water (····) and 70:30 ethanol/water (- · - ·). Sonication time of 600 s, acoustic amplitude 50 % and centrifugation at 9000 rpm for 15 min. Scan rate: 0.100 V s^{-1} . Supporting electrolyte 0.050 M phosphate buffer solution pH 7.40.

with the dispersions prepared using ethanol/water, either 70/30 or 50/50 v/v, the electrooxidation of AA is poorly defined, with two anodic peaks at -0.020 and 0.325 V . The peak at more negative potentials is due to the facilitated oxidation of AA at CNTs-modified surface while the other one corresponds to the oxidation of AA at bare GCE. In addition, the repeatability obtained with GCE/hMWCNT-PEI using PEI prepared in ethanol/water was poor compared to that for GCE modified with hMWCNT-PEI prepared in water. These results suggest a non-uniform deposition of CNTs at the electrode surface. Therefore, to obtain a homogeneous and stable film of hMWCNTs-PEI dispersion on the surface of GCE and a reproducible and well-defined voltammetric response of the redox marker, water was selected as solvent for preparing further dispersions.

3.1.2 Effect of Polyethyleneimine Concentration

CNT/polymer ratio is a very important parameter that influences the efficiency of the dispersions [13]. The polymer works as spacer between the nanotubes and modifies their potential energy due to the electrostatic repulsion. This energy barrier avoids the aggregation of the CNTs and makes possible to obtain CNTs dispersions in polar solvents [19].

Figure 2A displays the effect of PEI concentration on the Abs_{265} of the supernatant of the dispersions and on the electrochemical behavior of AA at the CNTs-modified GCE. The dispersions were prepared by sonication with the sonicator probe for 300 s by mixing 1.0 mg hMWCNTs with 1.0 mL PEI solutions of different con-

centrations from 0 to 5.0 mg mL^{-1} (prepared with water) followed by sonication for 300 s (with probe sonicator) and centrifugation at 9000 rpm for 15 min. The absorbance increases with PEI concentration, suggesting that the exfoliation process is more efficient as the polymer concentration increases, being 3.0 mg mL^{-1} the optimum value. The voltammetric behavior of GCE modified with the different dispersions was evaluated from the capacitive currents (Figure 2B) and the voltammetric parameters for AA electrooxidation (Figures 2C and 2D). As PEI concentration increases, there is an increment in the capacitive currents (Figure 2B) due to the presence of a higher amount of hMWCNTs in the supernatant of the dispersion. Figure 2C and D display the effect of PEI concentration on the electrochemical behavior of $1.0 \times 10^{-3} \text{ M}$ AA at GCE modified with the different hMWCNTs-PEI dispersions. There is an enhancement in the oxidation currents for AA (Figure 2C) up to 1.0 mg mL^{-1} PEI, and a shifting of E_p towards more negative values (Figure 2D) up to 3.0 mg mL^{-1} of PEI, concentration at which reaches the stationary values. Therefore, the effect of PEI concentration on the dispersion is not only connected with the increase in the electroactive area of the resulting GCE/hMWCNTs-PEI, but also with the catalytic activity of the dispersed CNTs. According to the results previously shown, 3.0 mg mL^{-1} PEI was selected for further experiments.

3.1.3 Effect of the Sonication Time and Acoustic Amplitude

The total energy (E) delivered by the ultrasonic processor produces changes in the number of cavitation events per volume. This energy not only depends on the applied power (P), fixed by the acoustic amplitude at the tip of the resonating probe, but also on the time (t) that the dispersion receives the ultrasonic treatment according to $E = P \times t$. Even when the separation of the nanotubes occurs in a very short period, longer times are required to produce a chain of cavitation events that guarantees the separation of the tubes, the diffusion of the polymer between the nanotubes and further interaction with them [42]. Hence, the study of the sonication time is an important aspect when preparing CNTs-polymers dispersions.

In this case the effect of the sonication time on the efficiency of hMWCNTs-PEI dispersions was also evaluated by UV-vis spectroscopy and cyclic voltammetry. Figure 3A shows the Abs_{265} of the supernatant of dispersions obtained by sonication of 1.0 mg mL^{-1} hMWCNTs with 3.0 mg mL^{-1} PEI in water for different times between 30 and 600 seconds followed by centrifugation at 9000 rpm for 15 min. The Abs_{265} increases with the ultracavitation time between 30 and 300 s to level off thereafter. For short sonication times, the absorbances are low since hMWCNTs that mainly exist as bundles are removed during the centrifugation step. When the sonication time increases, the mechanical energy minimizes the van der Waals interactions between the nanotubes walls. Conse-

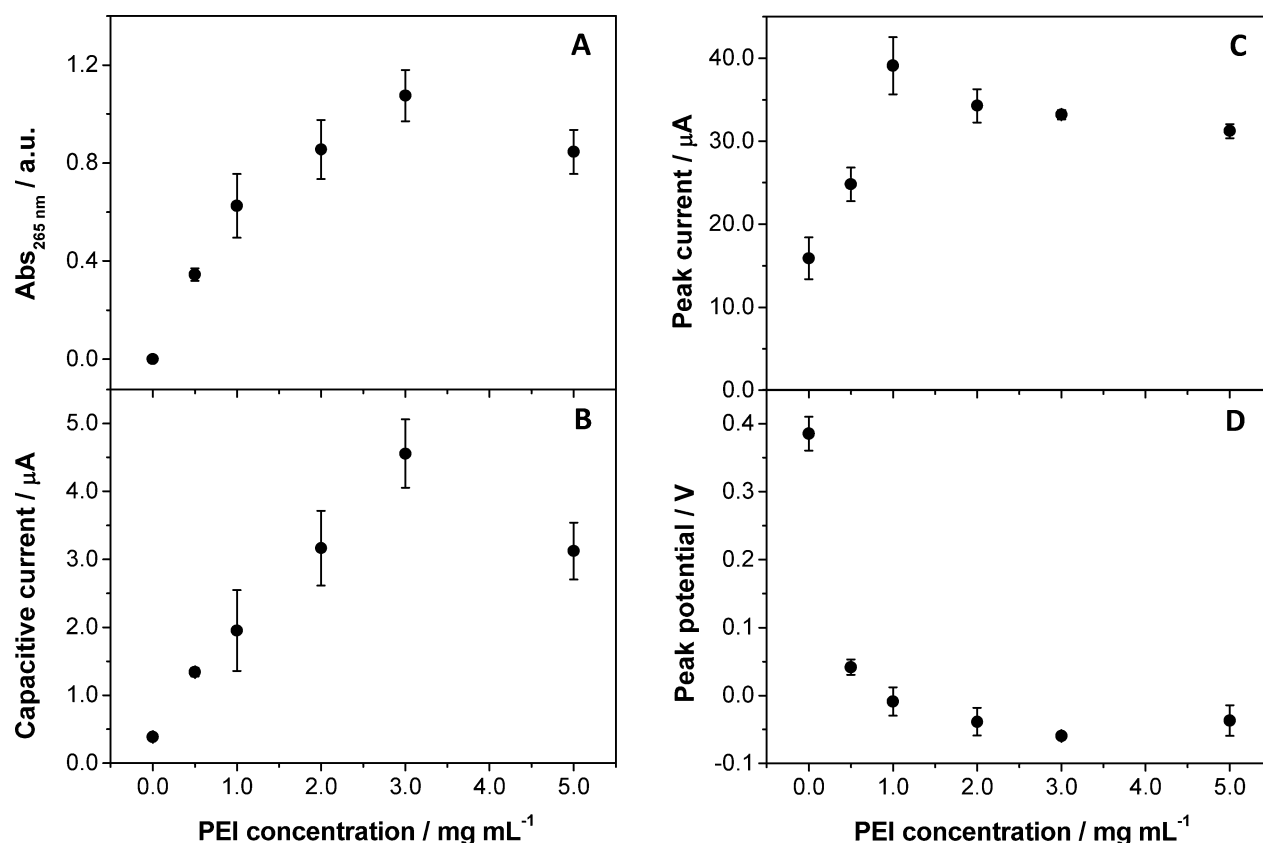


Fig. 2. Variation of (A) absorbances at 265 nm (B) capacitive currents; (C) peak currents and (D) peak potentials for 1.0×10^{-3} M AA oxidation, as a function of PEI concentration. The dispersions were prepared by mixing 1.0 mg mL^{-1} hMWCNTs in aqueous solutions of PEI of the desired concentration, followed by sonication for 300 s under acoustic amplitude of 50% and centrifugation at 9000 rpm for 15 min. The results correspond to the average of three dispersions. Other conditions as in Figure 1.

quently, Abs_{265} increases due to the increment of the individual nanotubes in the dispersion, indicating the improvement of the exfoliation process. The effect of the sonication time was also evaluated by cyclic voltammetry experiments at GCE/hMWCNTs-PEI. As Figure 3B displays, the capacitive currents increase with the ultracavitation time following the same tendency observed for the absorbancies in Figure 3A, reinforcing the conclusion that longer cavitation times exfoliate more nanotubes. The influence of the ultrasonication time on the electrooxidation of 1.0×10^{-3} M AA was evaluated from the analysis of the oxidation peak current (i_p) (Figure 3C) and peak potential (E_p) (Figure 3D). For short sonication periods, i_p increases with the ultracavitation time, reaching stationary values after 300 s. When the sonication time rises from 30 to 300 s, E_p shifts to more negative potentials, to remain constant thereafter. These results indicate that the electrooxidation of AA improves not only due to the increment of the electroactive area, but also due to the catalytic activity of CNTs, which is more efficient when the bundles are separated and the CNTs are wrapped by the polymer.

The increase of the acoustic amplitude from 50 to 70% produced a slight improvement of the amount of exfoliated nanotubes, without significant differences in the elec-

trochemical behavior of AA at GCE/hMWCNT-PEI (not shown). Taking into account that the increase of the sonicator horn amplitude can lead to significant changes in particle size distribution due to some reactions of the constituents, associative effects, nanotube damage, or reagglomeration [43], and considering that high sonication intensities could produce undesired side effects or breakage of CNTs, a sonication time of 300 s and acoustic amplitude of 50% were selected to obtain efficient CNT dispersions and very active GCE/hMWCNTs-PEI.

3.1.4 Effect of the Centrifugation

Table 1 summarizes the effect of the centrifugation of hMWCNT-PEI dispersions on the Abs_{265} and on the electroactive area of GCE modified with the dispersions. As the rotational speed increases during the centrifugation process, the Abs_{265} of the supernatants decreases. The electroactive areas decrease 42% and 66% when comparing GCE modified with the whole dispersion and GCE modified with the supernatant of the dispersion centrifuged at 4000 rpm or 9000 rpm, respectively. These results demonstrate that the centrifugation eliminates the bigger aggregates of CNTs and maintains the smaller ones and the individual CNTs wrapped by PEI.

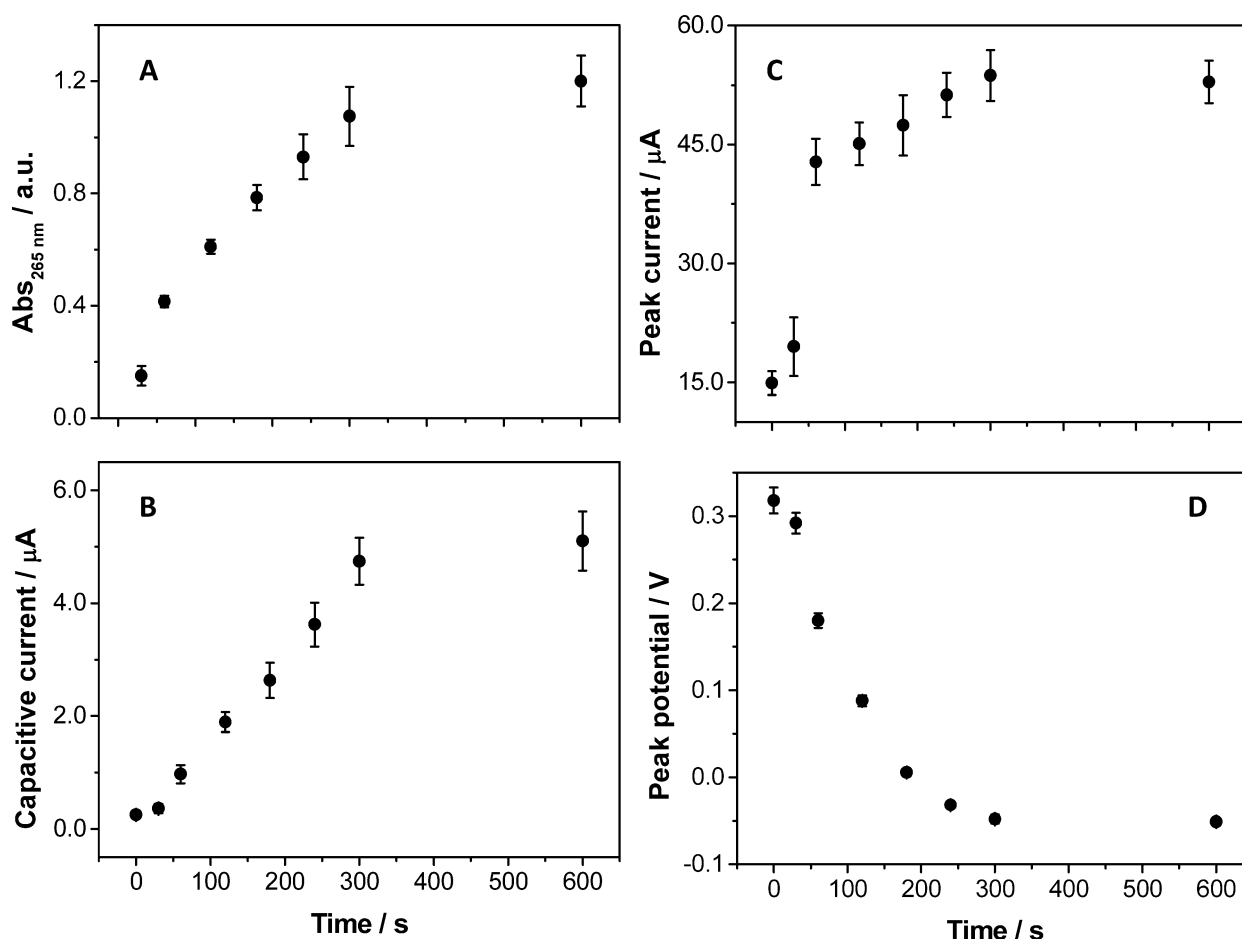


Fig. 3. Variation of (A) absorbances at 265 nm (B) capacitive currents; (C) peak currents and (D) peak potentials for 1.0×10^{-3} M AA oxidation, as a function of sonication time. The dispersions were obtained by mixing 1.0 mg mL^{-1} hMWCNTs in 3.0 mg mL^{-1} of aqueous PEI solutions, followed by sonication for different times (from 30 to 600 s) under acoustic amplitude of 50% and centrifugation at 9000 rpm for 15 min. Before performing the experiments the electrodes were cycled 15 times between -0.200 V and 0.800 V. The results correspond to the average of three dispersions. Other conditions as in Figure 1

Table 1. Absorbances at 265 nm and electrochemical areas for GCE modified with hMWCNTs-PEI dispersions as a function of the rotational speed. Dispersions conditions: 1.0 mg mL^{-1} hMWCNTs in 3.0 mg mL^{-1} PEI prepared in water; sonication time: 300 s; acoustic amplitude: 50%.

Acceleration force (rpm)	Abs _{265 nm} (a.u.)	Electrochemical surface
0	1.4 ± 0.2 [c]	0.398 ± 0.009
4000	1.2 ± 0.2 [b]	0.233 ± 0.008
9000	1.0 ± 0.2 [a]	0.134 ± 0.005

Dilutions: [a] 1:2; [b] 1:3; [c] 1:4

In agreement with these results, cyclic voltammograms for 1.0×10^{-3} M AA at GCE modified with the supernatant of the dispersion obtained after centrifugation for 15 min at 9000 rpm, present lower capacitive currents than those obtained at GCE modified with the whole dispersion, making possible a better definition of the oxidation current peak at -0.035 V (Figure 1-SI: Supporting Information). Therefore, it is clear that centrifugation of

the dispersion is necessary to obtain electrochemical sensors with low detection limits, high sensitivity and better peak definition.

3.1.5 Ultrasound Frequency: Bath vs. Probe Sonication

We compared the use of the ultrasonication bath and sonicator probe on the efficiency of hMWCNT-PEI dispersions prepared by different sonication times and centrifuged at 9000 rpm for 15 min. As it was previously shown in Figure 3, the saturation in the exfoliation process occurs after 300 s of treatment with sonicator probe. On the contrary, when using sonicator bath, the Abs₂₆₅ increased even after 120 min sonication and the maximum value was lower than the one obtained when using the sonicator probe, demonstrating that the amount of exfoliated nanotubes is smaller (not shown). These results are connected with the power dissipated using the different sonication protocols. For instance, if considering a sonication time of 600 s in both cases, the power per volume

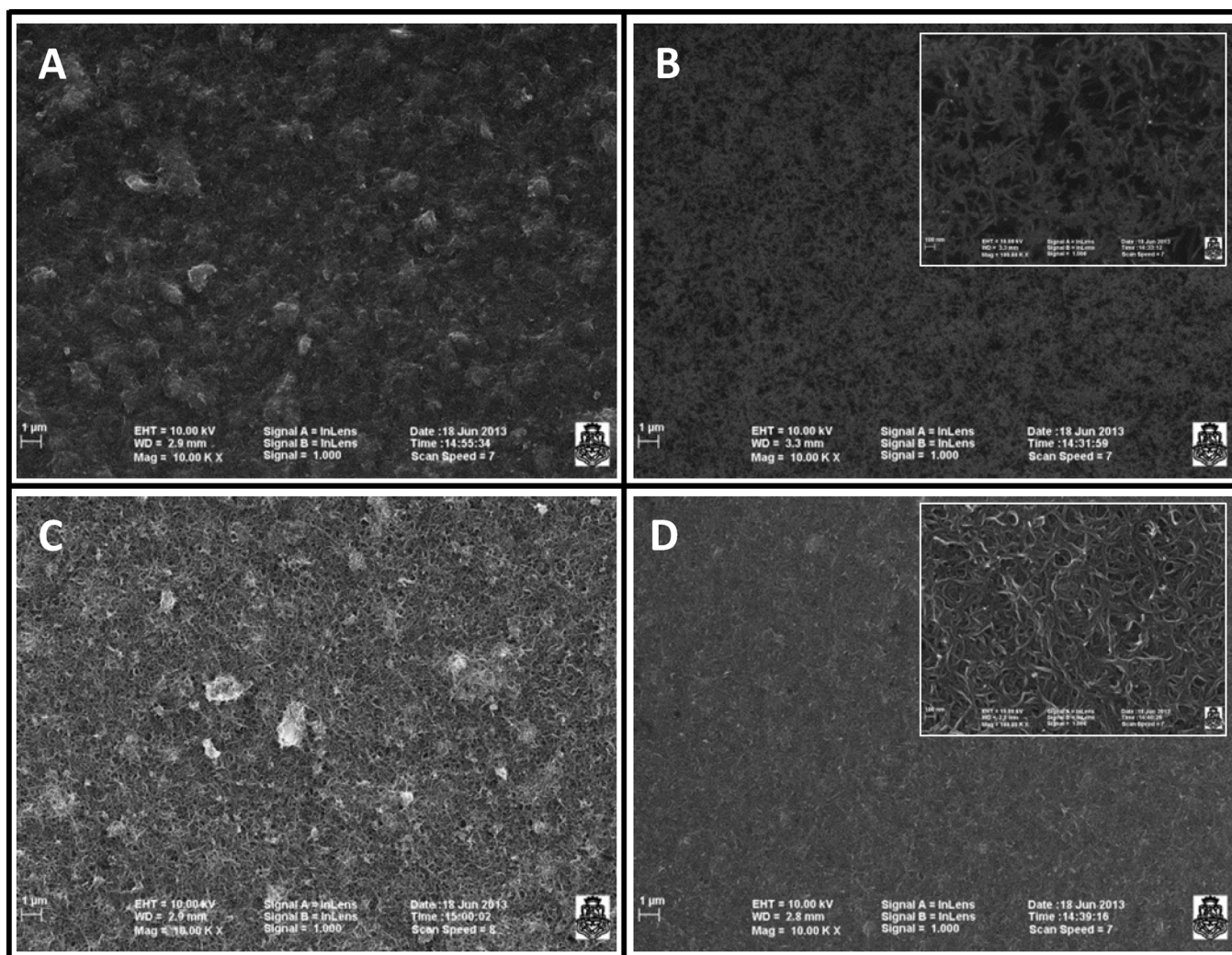


Fig. 4. SEM micrographs of glassy carbon disks modified with dispersions of hMWCNTs-PEI (A, B) and bMWCNTs (C, D) without (A, C) and with (B, D) centrifugation at 9000 rpm for 15 min. Magnification: 10000 \times . The insets in B and D correspond to pictures of the same disk obtained with higher magnification (100000 \times).

dissipated with the sonicator probe is around 60 times higher than the one dissipated using the sonicator bath.

The i_p for 1.0×10^{-3} M AA oxidation obtained from cyclic voltammograms at GCE modified with the supernatant of hMWCNTs-PEI dispersions prepared using 15 min sonication with sonicator probe or ultrasonic bath were 62.4 μ A and 15.4 μ A, respectively, demonstrating once more the advantages of ultracavitation on the efficiency of the dispersion (not shown).

Considering that the sonicator probe operates at lower frequencies and that a decrease in the frequency is responsible for longer acoustic periods, higher bubble size and more cavitation intensity; it is clear that the increase in the rate of exfoliation achieved with this sonicator is due to the delivery of high energy to the CNTs [35]. In addition, in this case the waves are directly delivered to the CNT samples, while those produced by the sonicator bath must cross the walls of the tube that contains the dispersion [43].

3.2 Hollow vs. Bamboo-Like MWCNT-PEI Dispersions

To evaluate the influence of MWCNT structure on the efficiency of the resulting dispersions, we compare dispersions obtained by mixing 1.0 mg bMWCNT or 1.0 mg hMWCNT in 1.0 mL of 3.0 mg mL⁻¹ PEI prepared in water by applying 50% of amplitude for different sonication times and centrifugation at 9000 rpm for 15 min. The Abs₂₆₅ for the supernatants increases with the sonication time due to the increment of exfoliated nanotubes, although the rate of increase is higher for bMWCNTs-PEI (Figure 2A-SI: Supporting Information). The comparison of the CVs obtained for GCE modified with bMWCNT-PEI and hMWCNT displays a similar trend, with faster increase of the capacitive currents (Figure 2B-SI: Supporting Information) and AA electrooxidation currents (Figure 2C-SI: Supporting Information) for GCE/bMWCNT-PEI. Regarding the variation of E_p for AA oxidation with the sonication time, (Figure 2D-SI: Supporting Information), the shifting to less positive values is faster in the

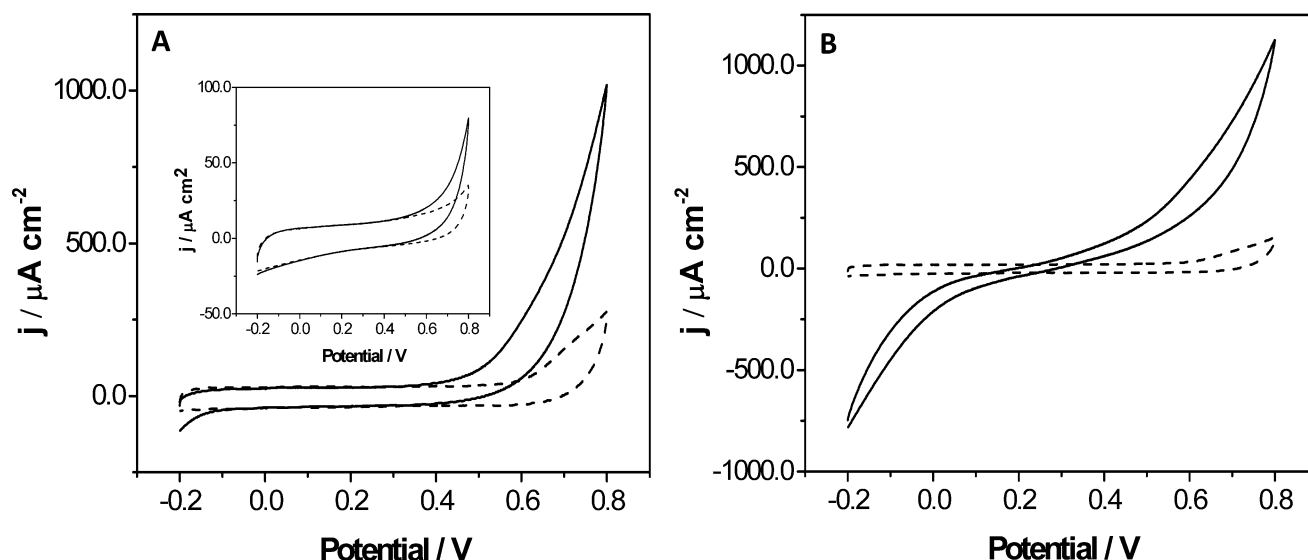


Fig. 5. Cyclic voltammograms for 1.0×10^{-2} M hydrogen peroxide (solid line) and 0.050 M phosphate buffer solution pH 7.40 (dashed line) obtained at GCE modified with (A) hMWCNTs-PEI and (B) bMWCNTs-PEI dispersions. The inset of Figure 5A corresponds to the cyclic voltammograms obtained at bare GCE. Scan rate: 0.100 V s^{-1} . The dispersions were obtained by mixing 1.0 mg mL^{-1} hMWCNTs in 3.0 mg mL^{-1} of aqueous PEI solutions sonicated for 300 s under acoustic amplitude of 50% and centrifuged at 9000 rpm for 15 min. Before the experiments the electrodes were cycled 15 times between -0.200 V and 0.800 V .

case of GCE/bMWCNTs-PEI where the lowest E_p was reached after 30 s sonication. Both parameters reach the same maximum value than at GCE/hMWCNTs-PEI. The effect of polymer concentration was also evaluated, using AA as redox marker, although no significant differences were observed either in i_p or E_p (not shown). Therefore, selecting 300 s of sonication, it is possible to obtain the same Abs_{265} , capacitive currents, and i_p and E_p for AA electrooxidation using either GCE/bMWCNT-PEI or GCE/hMWCNT-PEI.

Figure 4 shows SEM micrographs of glassy carbon disks modified with hMWCNTs-PEI (A, B) and bMWCNTs-PEI (C, D) prepared under the selected conditions (1.0 mg mL^{-1} MWCNTs in 3.0 mg mL^{-1} PEI (in water) at an acoustic amplitude of 50% for 300 s). In all cases the dispersions cover the whole disk surface. The images for the non-centrifuged samples show a great number of CNTs aggregates (A, C). On the contrary, after centrifuging for 15 min at 9000 rpm, there is an important decrease in the number of aggregates (B, D) and the coverage is more homogeneous. The Insets show the centrifuged samples at higher magnification ($100\,000\times$) where is possible to see more clearly the distribution of MWCNTs on the glassy carbon surface.

3.3 Analytical Applications of the Optimized MWCNT-PEI Dispersions: Quantification of Hydrogen Peroxide

Figure 5 shows cyclic voltammograms obtained at GCE/hMWCNTs-PEI (A) and GCE/bMWCNTs-PEI (B) in a 0.050 M phosphate buffer solution pH 7.40 without (dotted line) and with (solid line) 1.0×10^{-2} M H_2O_2 . Compared to bare GCE (Inset of Figure 5A), at GCE/

hMWCNTs-PEI there is a decrease in the overvoltages for the oxidation and reduction of hydrogen peroxide. In fact, the oxidation of hydrogen peroxide starts at 0.400 V while the reduction starts at -0.100 V . At GCE/bMWCNTs-PEI, the overvoltages for the oxidation and reduction of the redox marker decrease around 100 mV and 300 mV, respectively, compared to GCE/hMWCNT-PEI. In addition to this drastic decrease in the oxidation and reduction overvoltages, there is a noticeable increase in the oxidation and reduction currents, indicating that, as it was previously shown for AA, the presence of the edge-like defects regularly located along the walls of bMWCNTs largely improves the catalytic activity compared to hMWCNTs [3,4].

Figure 6A displays the amperometric recordings obtained at 0.400 V at GCE/bMWCNTs-PEI (a) and GCE/hMWCNTs-PEI (b) for successive additions of hydrogen peroxide. In agreement with the voltammetric results presented in Figure 5, a well-defined, faster (electrodes response time 2.5 vs. 5 seconds, respectively) and more sensitive response is observed in the case of GCE/bMWCNT-PEI. Figure 6Ba and the Inset b show the calibration plots for hydrogen peroxide obtained from the amperometric recordings shown in Figure 6A. The amperometric response of hydrogen peroxide at GCE/bMWCNT-PEI at 0.100 V is shown in Figure 6C. A fast and sensitive reduction of hydrogen peroxide is observed (response time 3.0 seconds) in this case, at variance with GCE/hMWCNT-PEI where the amperometric signal is negligible at this potential (not shown). Figure 6D displays the calibration plot for the results shown in Figure 6C. The regression curve obtained at 0.400 V are $y = (2.09 \pm 0.02) \times 10^3 (\mu\text{A M}^{-1}) [\text{H}_2\text{O}_2] (\text{M})$ ($r = 0.998$) for

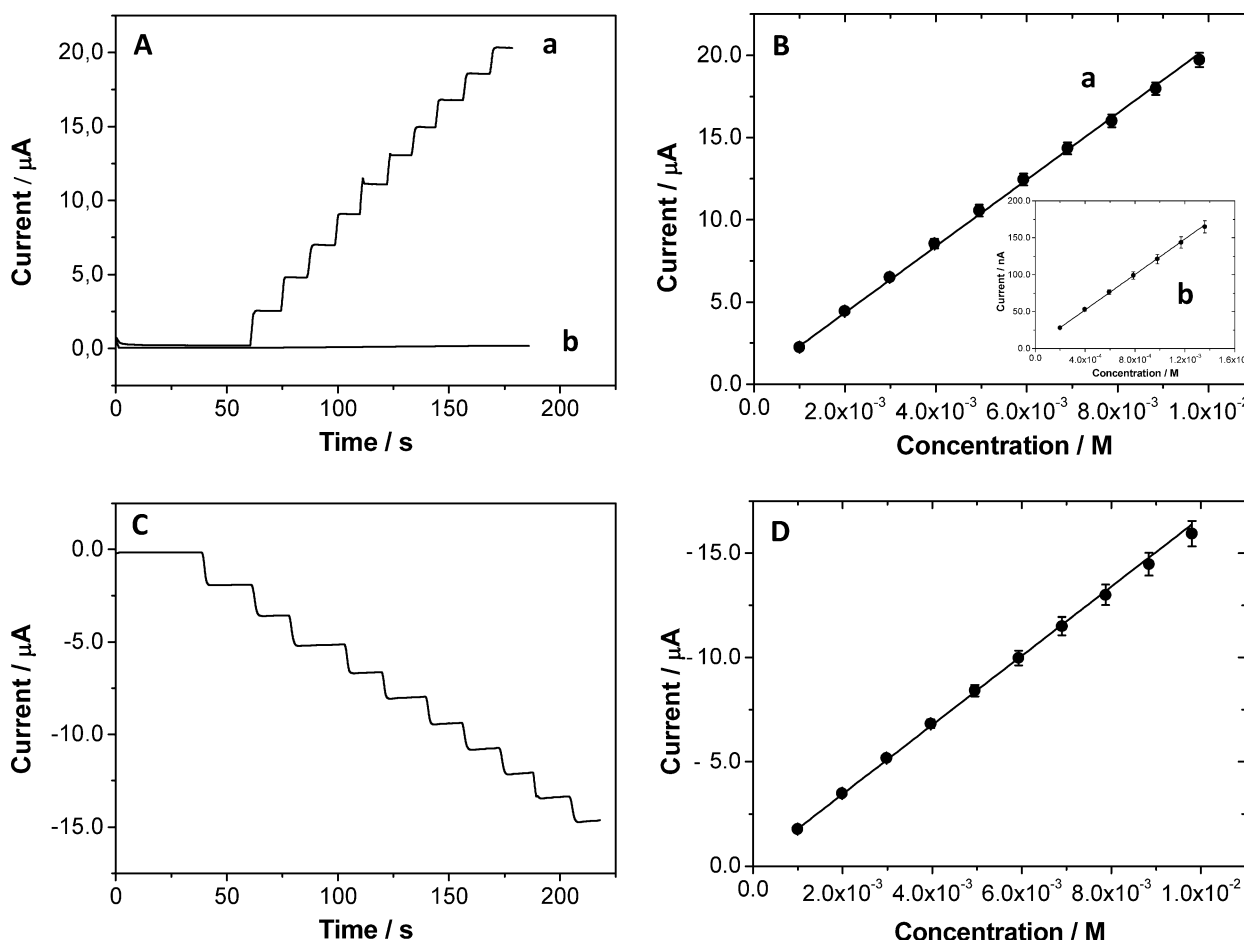


Fig. 6. (A) Amperometric responses obtained at 0.400 V for successive additions of hydrogen peroxide at GCE/bMWCNTs-PEI (a) and GCE/hMWCNTs-PEI (b); (B) Calibration plots obtained from the amperometric recordings shown in Figure 6A; (C) Amperometric recording for successive additions of hydrogen peroxide at GCE/bMWCNTs-PEI obtained at 0.100 V; (D) Calibration plot obtained from the amperometric recording shown in Figure 6C. The preparation of the dispersions and the other conditions are the same as in Figure 5.

bMWCNTs and $y = (0.128 \pm 0.002) \times 10^3 (\mu\text{A M}^{-1}) [\text{H}_2\text{O}_2]$ (M) ($r = 0.997$) for hMWCNT. At 0.100 V the regression curve is $y = (-1.72 \pm 0.02) \times 10^3 (\mu\text{A M}^{-1}) (r = 0.9991)$ for bMWCNTs. The detection limits obtained at GCE/bMWCNT-PEI at 0.100 V and 0.400 V are 5.5 μM and 3.6 μM , respectively, while the corresponding detection limit at GCE/hMWCNT-PEI and 0.400 V is 45 μM , demonstrating the advantages of the bMWCNTs mainly in the reduction of hydrogen peroxide.

As the electroactive area of GCE modified with the dispersion containing bMWCNTs and hMWCNTs are different, it is interesting to compare the sensitivity normalized by the area, the values of sensitivity per cm^2 are $(11.9 \pm 0.1) \times 10^3 \mu\text{A M}^{-1} \text{cm}^{-2}$; $(0.96 \pm 0.01) \times 10^3 \mu\text{A M}^{-1} \text{cm}^{-2}$ and $(9.8 \pm 0.1) \times 10^3 \mu\text{A M}^{-1} \text{cm}^{-2}$ for GCE/bMWCNTs-PEI (Figure 6 curve a), GCE/hMWCNTs-PEI (curve b), and GCE/bMWCNTs-PEI at 0.100 V (Figure 6 curve c); respectively. These values clearly confirm the advantages of the bMWCNTs; at this surface the normalized sensitivity is 12 times higher than the observed at hMWCNT at 0.400 V.

The reproducibilities for amperometric experiments performed at 0.400 V with GCE/hMWCNTs-PEI and GCE/bMWCNTs-PEI, obtained with five different dispersions and three electrodes for each dispersion, were 7.8% and 6.1%, respectively. The repeatability, evaluated with five electrodes modified with the same dispersion was 5.1% for GCE/hMWCNTs-PEI and 1.7% for GCE/bMWCNTs-PEI. The results indicate that the reproducibility is excellent in both cases.

The stability of hMWCNTs-PEI and bMWCNTs-PEI dispersions maintained at room temperature was also evaluated from amperometric experiments performed at 0.400 V using GCE modified with these dispersions. After 15 days, the sensitivity remained around 95% of the original value in the case of both electrodes, indicating an excellent stability.

Hydrogen peroxide was quantified in a mouthwash sample using both electrodes, GCE/bMWCNT-PEI and GCE/hMWCNT-PEI. As described in Section 2.4, only a convenient dilution with phosphate buffer solution was performed before transferring the sample to the electro-

Table 2. Determination of H₂O₂ in a mouthwash sample.

CNT dispersion	E_{app} (V)	H ₂ O ₂ (% w/v)		RSD (%)	Recovery (%)
		Reported	Found		
hMWCNT _{9000 rpm}	+0.5	1.50	1.49 ± 0.06	3.8	99 ± 4
bMWCNT _{9000 rpm}	+0.4	1.50	1.49 ± 0.02	1.6	99 ± 2
bMWCNT _{9000 rpm}	+0.1	1.50	1.48 ± 0.03	2.3	99 ± 2

chemical cell. In order to minimize matrix effect, the determination of hydrogen peroxide was accomplished by using the standard addition method. Table 2 summarizes the hydrogen peroxide concentrations obtained with GCE/bMWCNTs-PEI at 0.400 V, GCE/hMWCNTs-PEI at 0.500 V (to improve the sensitivity) and GCE/bMWCNTs-PEI at 0.100 V, demonstrating an excellent agreement with the labeled values, with errors lower than 5.0 % in all cases. These results demonstrate the suitability of GCE electrodes modified with hMWCNTs-PEI and bMWCNTs-PEI dispersions for the reliable analysis of hydrogen peroxide in mouthwash samples. Even when both electrodes can be successfully used for the quantification of this analyte, GCE/bMWCNT-PEI present the great advantage of allowing the determination at very low potentials.

4 Conclusions

Spectroscopic and electrochemical studies demonstrated that the adequate combination of optimized ultracavitation and centrifugation allows obtaining successful dispersions and, consequently, MWCNTs-PEI modified-GCE with low capacitive currents and excellent resolution of the different faradaic processes.

The comparison of bMWCNT and hMWCNT-PEI dispersions revealed that bMWCNT are dispersed faster than hMWCNT and the resulting modified GCE presented enhanced kinetics for the oxidation and reduction of hydrogen peroxide compared to GCE/hMWCNTs-PEI due to the presence of the defects regularly located along the walls of the bMWCNTs, allowing the sensing of this compound at considerably lower potentials in a more sensitive way.

In summary, a critical analysis of the different experimental conditions is absolutely necessary when dispersing CNTs with polymers in order to obtain an efficient dispersion that once deposited onto the electrode surfaces makes possible to obtain a homogeneous and robust deposit and sensitive sensing of different analytes.

Acknowledgements

The authors thank CONICET, SECyT-UNC, ANPCyT, MINCyT-Córdoba for the financial support. M. E. acknowledges CONICET for the fellowship.

References

- [1] A. Walcarius, S. D. Minter, J. Wang, Y. Lin, A. Mercoci, *J. Mater. Chem. B* **2013**, 1, 4878.
- [2] C. I. L. Justino, T. A. P. Rocha-Santos, A. C. Duarte, *Trends Anal. Chem.* **2013**, 45, 24.
- [3] A. Jorio, M. S. Dresselhaus, G. Dresselhaus, *Topics in Applied Physics, Volume 111, Carbon Nanotubes, Advanced Topics in the Synthesis, Structure, Properties, and Applications*, Springer, Heidelberg **2008**.
- [4] R. L. Mccreery, *Chem. Rev.* **2008**, 108, 2646.
- [5] L. Y. Heng, A. Chou, J. Yu, Y. Chen, J. J. Gooding, *Electrochem. Commun.* **2005**, 7, 1457.
- [6] K. Matsubara, K. Waki, *Electrochim. Acta* **2010**, 55, 9166.
- [7] S. Shanmugann, A. Gedanken, *Electrochem. Commun.* **2006**, 8, 1099.
- [8] S. Shanmugann, A. Gedanken, *J. Phys. Chem. B* **2006**, 110, 2037.
- [9] E. N. Primo, P. Cañete-Rosales, S. Bollo, M. D. Rubianes, G. A. Rivas, *Colloid Surf. B* **2013**, 108, 329.
- [10] Z. Zhu, J. Wang, A. Munir, H. S. Zhou, *Colloid Surf. A* **2011**, 385, 91.
- [11] L. Gan, R. Lv, H. D. Du, B. H. Li, F. Y. Kang, *Carbon* **2009**, 47, 1883.
- [12] Z. Zhu, J. Wang, A. Munir, H. S. Zhou, *Electrochim. Acta* **2010**, 55, 8517.
- [13] E. N. Primo, F. A. Gutierrez, G. L. Luque, P. R. Dalmasso, A. Gasnier, Y. Jalit, M. Moreno, M. V. Bracamonte, M. Eguilaz Rubio, M. L. Pedano, M. C. Rodríguez, N. F. Ferreyra, M. D. Rubianes, S. Bollo, G. A. Rivas, *Anal. Chim. Acta* **2013**, 805, 19.
- [14] T. Premkumar, R. Mezzenga, K. E. Geckeler, *Small* **2012**, 8, 1299.
- [15] S. W. Kim, T. Kim, Y. S. Kim, H. S. Choi, H. J. Lim, S. J. Yang, C. R. Park, *Carbon* **2012**, 50, 3.
- [16] C. Gao, Z. Guo, J. H. Liu, X. J. Huang, *Nanoscale* **2012**, 4, 1948.
- [17] P. Bilalis, D. Katsigiannopoulos, A. Avregopoulos, G. Sakellariou, *RSC Advances* **2014**, 4, 2911.
- [18] D. Tuncel, *Nanoscale* **2011**, 3, 3545.
- [19] M. Zhang, A. Smith, W. Gorski, *Anal. Chem.* **2010**, 82, 1299.
- [20] P. C. Ma, N. A. Siddiqui, G. Marom, J. K. Kim, *Composites: Part A* **2010**, 41, 1345.
- [21] X. Ling, Y. Wei, L. Zou, S. Xu, *Colloids Surf. B, Physicochem. Eng. Asp.* **2014**, 443, 19.
- [22] M. Eguilaz, R. Villalonga, P. Yáñez-Sedeño, J. M. Pingarrón, *Anal. Chem.* **2011**, 83, 7807.
- [23] S. Wang, D. Yu, L. Dai, *J. Am. Chem. Soc.* **2011**, 133, 5182.
- [24] M. Zhang, A. Smith, W. Gorski, *Anal. Chem.* **2004**, 76, 5045.
- [25] M. D. Rubianes, G. A. Rivas, *Electrochem. Commun.* **2007**, 9, 480.
- [26] A. Sánchez-Arribas, E. Bermejo, M. Chicharro, A. Zapardiel, G. L. Luque, N. F. Ferreyra, G. A. Rivas, *Anal. Chim. Acta* **2007**, 596, 183.

- [27] M. C. Rodríguez, M. D. Rubianes, G. A. Rivas, *J. Nanosci. Nanotechnol.* **2008**, *8*, 6003.
- [28] G. L. Luque, N. F. Ferreyra, A. Granero, S. Bollo, G. A. Rivas, *Electrochim. Acta* **2011**, *56*, 9121.
- [29] M. Shim, A. Javey, N. W. Sh. Kam, H. Dai, *J. Am. Chem. Soc.* **2001**, *123*, 11512.
- [30] Y. -T. Shieh, T. Yu, T. L. Wang, Ch. H. Yang, *J. Electroanal. Chem.* **2012**, *664*, 139.
- [31] M. A. Correa-Duarte, L. M. Liz-Marzán, *J. Mater. Chem.* **2006**, *16*, 22.
- [32] H. Yu, S. Hermann, S. E. Schulz, T. Gessner, Z. Dong, W. J. Li, *Chem. Phys.* **2012**, *408*, 11.
- [33] Q. Cheng, S. Debnath, E. Gregan, H. J. Byrne, *J. Phys. Chem. C* **2010**, *114*, 8821.
- [34] T. Yasumitsu, G. Liu, J. M. Leveque, S. Aonuma, L. Duclaux, T. Kimura, N. Komatsu, *Ultrason. Sonochem.* **2013**, *20*, 37.
- [35] A. J. Blanch, C. E. Lenehan, J. S. Quinton, *Carbon* **2011**, *49*, 5213.
- [36] J. J. Gooding, V. G. Praig, E. A. H. Hall, *Anal. Chem.* **1998**, *70*, 2396–2402.
- [37] S. Daniel, T. P. Rao, K. S. Rao, S. U. Rani, G. R. K. Naidu, H. Y. Lee, T. Kawai, *Sens. Actuators B* **2007**, *122*, 672.
- [38] Y. Liu, L. Yu, S. Zhang, J. Yuan, L. Shi, L. Zheng, *Colloid Surf. A* **2010**, *359*, 66.
- [39] Z. Wu, W. Feng, Y. Feng, Q. Liu, X. Xu, T. Sekimo, A. Fujii, M. Ozaki, *Carbon* **2007**, *45*, 1212.
- [40] J. Yu, N. Grossiord, C. E. Koning, J. Loos, *Carbon* **2007**, *45*, 618.
- [41] F. Lu, S. Zhang, L. Zheng, *J. Mol. Liq.* **2012**, *173*, 42.
- [42] Y. Y. Huang, E. M. Terentjev, *Int. J. Mater. Form.* **2008**, *1*, 63.
- [43] T. R. Fromyr, F. H. Housey, T. Olsen, *J. Nanotechnol.* **2012**, Article ID 545930, doi 10.1155/2012/545930.

Received: June 13, 2014

Accepted: August 1, 2014

Published online: ■■ ■■, 2014

FULL PAPERS

M. Eguílaz, N. F. Ferreyra,*
G. A. Rivas*

■■■ – ■■■



Dispersions of Hollow and Bamboo-Like Multiwalled Carbon Nanotubes in Polyethyleneimine: Critical Analysis of the Preparation Conditions and Applications for Electrochemical Sensing

